

## **3. MATERIALS AND METHODS**

## 3.1 Materials

The raw materials used in this work are only partially composed of individual chemical substances. Especially in the case of surfactants, their composition may vary depending on the manufacturer. Therefore, the producer details are mentioned for all materials used.

### 3.1.1 Buparvaquone

Buparvaquone (BPQ) (trans-2-[4-tert-butylcyclohexylmethyl]-3-hydroxy-1,4-naphthoquinone), belongs to the group of the naphthoquinones. It is a relatively small molecule with a molecular weight of 326 g/mol. See structure in Figure 3-1. Naphthoquinones are interesting compounds mainly due to their antimicrobial and fungicidal properties (Kayser and Kiderlen 2003). As many other substances with pharmaceutical effect, several naphthoquinones are very poorly water soluble and lipophilic molecules, a fact frequently associated to a low bioavailability of drugs with a dissolution rate-limiting step to absorption. BPQ is a yellow crystalline powder with a melting range of 174–184 °C. BPQ is a weakly acid 1,4-naphthoquinone (pKa 5.2), highly lipophilic (LogP = 6.5) and therefore processing a very low aqueous solubility ( $\leq 0.03 \mu\text{g/mL}$  at 25 °C). The drug is soluble in chloroform, sparingly soluble in methylene chloride and slightly soluble in methanol. The formulation of BPQ in order to improve its solubility rate is attractive due to the number of therapeutical applications associated to this drug. Effectiveness of BPQ has been described against causal pathogens of diseases like malaria (Martin, Bustard et al. 1973), cryptosporidiosis (Kayser 2001), leishmaniasis (Croft, Hogg et al. 1992) and *Pneumocystis carinii* pneumonia (main causal of pneumonia in AIDS and immunosuppressed patients) (Kaneshiro, Sul et al. 2001). The mechanism of action of the drug has not been fully elucidated. In analogy to atovaquone and other 1,4-naphthoquinones, buparvaquone most likely acts via a mechanism involving the inhibition of electron transport in the mitochondria by binding to the pathogens' *bc<sub>1</sub>* complex (Fry, Hudson et al. 1984). In the particular case of *P. carinii* there seems to be more than one mechanism of action of the drug. The effect of buparvaquone and other naphthoquinones on the ubiquinone (Q<sub>10</sub>) biosynthesis has also been described (Kaneshiro, Sul et al. 2000; Kaneshiro, Basselin et al. 2006).

BPQ was developed in the 80's (Hudson and Randall 1982). Since that time, it was extensively tested for veterinary use against *Theileria annulata* (Tropical theileriosis),

*T. parva* (East Coast Fever) (Hudson, Randall et al. 1985; McHardy, Wekesa et al. 1985; Dhar, Malhotra et al. 1986; Wilkie, Brown et al. 1998) and *T. sergenti* (Minami, Nakano et al. 1985), both in laboratory studies and in field trials, and it has undergone a rigorous programme of toxicology and safety studies. BPQ has been formulated as a solution for intramuscular injection (Butalex<sup>TM</sup>, Coopers Animal Health Ltd, Berkhamsted, Herts, UK) using an organic solvent as dissolution medium. The formulation offers a safe and convenient alternative for the treatment of theileriosis in cattle. BPQ has not been commercialized for human use. The secondary effects following BPQ therapy has not been reported. The acute toxicity of the drug administered in rats has shown an oral LD<sub>50</sub> >8000 mg/kg (McHardy 1988).

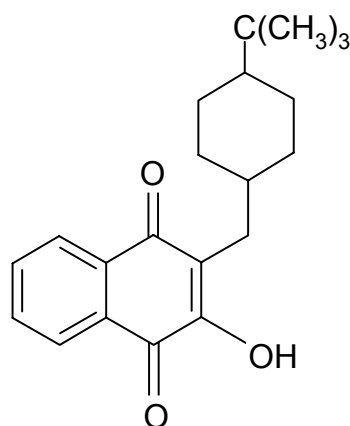


**Figure 3-1: Chemical structure of buparvaquone**

To date, several attempts have been made in order to improve the solubility of the drug. Nanosuspensions with enhanced mucoadhesive properties were prepared to be used against *Cryptosporidium parvum* (Jacobs, Kayser et al. 2001). The formulation has shown effectivity in intestinal *Cryptosporidium* infections (Kayser 2001). The activity of BPQ against cutaneous and visceral leishmaniasis (Croft, Hogg et al. 1992), makes the molecule attractive for further pharmaceutical development. Recently a synthesis of novel water-soluble phosphate prodrugs of BPQ has been published. The most potential prodrug during in vitro test was found to be the phosphonoxymethyl-buparvaquone-oxime, with high aqueous solubility and good chemical stability (Mäntylä, Garnier et al. 2004; Mäntylä, Rautio et al. 2004).

The BPQ used in this work was kindly provided by the company Innova-Specialties, Inc. (Missouri, USA). An additional batch of BPQ was used as an external reference substance for quantification and method validation purposes. This was provided by the company Essex Animal Health Friesoythe (Friesoythe, Germany). BPQ for the

initial formulation tests was donated by Dr. Simon L. Croft from the London School of Tropical Medicine (London, United Kingdom).

### 3.1.2 Atovaquone

Atovaquone (ATQ) (trans-2-[4-(4-chlorophenyl)cyclohexyl]-3-hydroxy-1,4-naphthalenedione. ATQ is an analog of protozoan ubiquinone, a mitochondrial protein involved in electron transport. ATQ interacts and irreversibly binds to cytochrome *b* in the *bc*<sub>1</sub> complex within the mitochondria, disrupting the electron transport inhibiting the oxidative phosphorylation and the synthesis of ATP in the targeted pathogen. The chemical structure of the molecule can be seen in Figure 3-2.

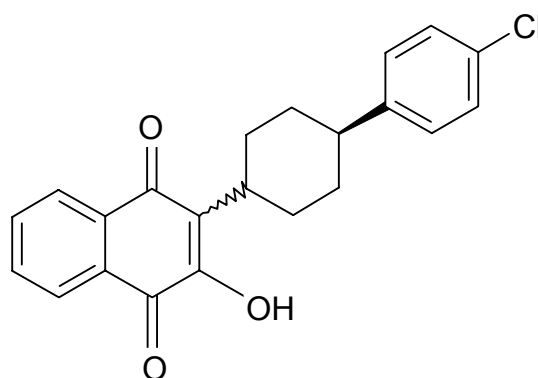


**Figure 3-2: Chemical structure of atovaquone**

It is a drug with broad spectrum antiprotozoal activity (Hudson, Randall et al. 1985). It is effective for the treatment and prevention of *Pneumocystis carinii* pneumonia (PcP) (Hughes, Gray et al. 1990), malaria (Chiodini, Conlon et al. 1995) and toxoplasmosis (Araujo, Huskinson et al. 1991; Schöler, Krause et al. 2001). For this work ATQ was particularly relevant due to its use against PcP. In the case of mild-to-moderate *Pneumocystis* pneumonia, although the combination of trimethoprim and sulfamethoxazole (TMP/SMX) is the first-line prophylactic and therapeutic agent, ATQ was approved in 1992 by the Food and Drug Administration (FDA) for the oral treatment of patients for whom the standard treatment is intolerable or ineffective (Hughes, Leoung et al. 1993; El-Sadr, Murphy et al. 1998; Chan, Montaner et al. 1999; U.S. Public Health Service and Infectious Diseases Society of America Prevention of Opportunistic Infections Working Group 2002). ATQ is a yellow crystalline solid practically insoluble in water. The drug is now commercialized as an oral suspension by the company GlaxoSmithKline with the names Wellvone<sup>®</sup> and Mepron<sup>®</sup>. The suspension is a formulation of micro-fine particles, with reduced size to

facilitate the absorption. The recommended dose in the prevention of PcP is 1500 mg daily. In the treatment of mild-to-moderate PcP the recommended oral dose is 750 mg twice daily for 21 days (GlaxoSmithKline 2001). This formulation was donated by GlaxoSmithKline (Munich, Germany) and used as a therapy during the animal tests conducted in mice. The group receiving this formulation was designed as positive control group.

### 3.1.3 Parvaquone

Parvaquone (2-cyclohexyl-3-hydroxy-1,4-naphthoquinone) is a yellow crystalline powder. It was donated by the company Cross Vetpharm Group Ltd. (Dublin, Ireland). The drug was used in this work only as internal standard for the HPLC methodology. Parvaquone was selected for being a structurally similar analogue of buparvaquone and specific to PcP therapy. The structure of the molecule is shown in Figure 3-3. The drug is currently only of veterinary use in the treatment of theileriosis. It is not prescribed for human use. This is particularly important in possible further utilization of the method for the quantification of the drug in biological samples (see 3.2.4.5).

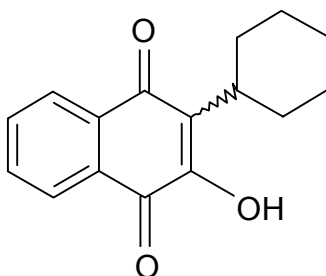


**Figure 3-3: Structural formula of parvaquone**

### 3.1.4 Emulsifying agents

In the preparation of aqueous nanosuspensions to be delivered by means of a nebulizer system, surface active ingredients are of particular relevance not only enhancing the colloidal stability of the formulation, by decreasing the rate of coalescence and nanocrystals aggregation, but also lowering the interfacial tension between two immiscible phases. By reducing the surface tension values of aqueous dispersion media, surfactants are able to improve the aerosolization properties of the formulation (see part 2.5.2.).

Some polymers have also surface-active properties (e.g. PVA, see below), which is due to the dual nature of the structure, composed mainly for both hydrophobic and hydrophilic chemical substituents. Non-ionic surfactants were selected for this work, for being less irritant than anionic or cationic surfactants for pulmonary use. Non-ionic surfactants act mainly through steric stabilization of the colloidal systems. Non-ionic surfactants can be classified according to their hydrophilic-lipophilic balance (HLB), which is an arbitrary scale of values denoting the relative affinity of the surfactant for oil and water. Lipophilic surfactants have low HLB values (less than 10) and are good antifoaming and wetting agents, while hydrophilic surfactants (HLB>10) are for example used as solubilising agents (Sweetman 2004).

#### 3.1.4.1 Tyloxapol®

Tyloxapol is a liquid polymer of 4-(1,1,3,3-tetramethylbutyl)phenol with ethylene oxide and formaldehyde. The surfactant was purchased from Sigma-Aldrich (Deisenhofen, Germany). It is a viscous amber liquid, sometimes slightly turbid, with a slight aromatic odour. It is a non-ionic surfactant of the alkyl aryl polyether alcohol type with a HLB value of 12.5. Solutions have been used as an aqueous inhalation as a mucolytic for tenacious bronchopulmonary secretions and as a vehicle for aerosol medication (Sweetman 2004). The medicament Tacholiquin® (Bene Arzneimittel GmbH, Munich, Germany) is a 1% or 0.1% tyloxapol solution recommended as a mucolytic in patients who simultaneously receive treatment with antibiotics, or corticoids (bene Arzneimittel GmbH 1995). The product SuperVent™ from the company Discovery Laboratories, Inc. (Pennsylvania, USA) is also a mucolytic recommended mainly for patients suffering from cystic fibrosis. The chemical structure of the tyloxapol molecule is shown in Figure 3-4.

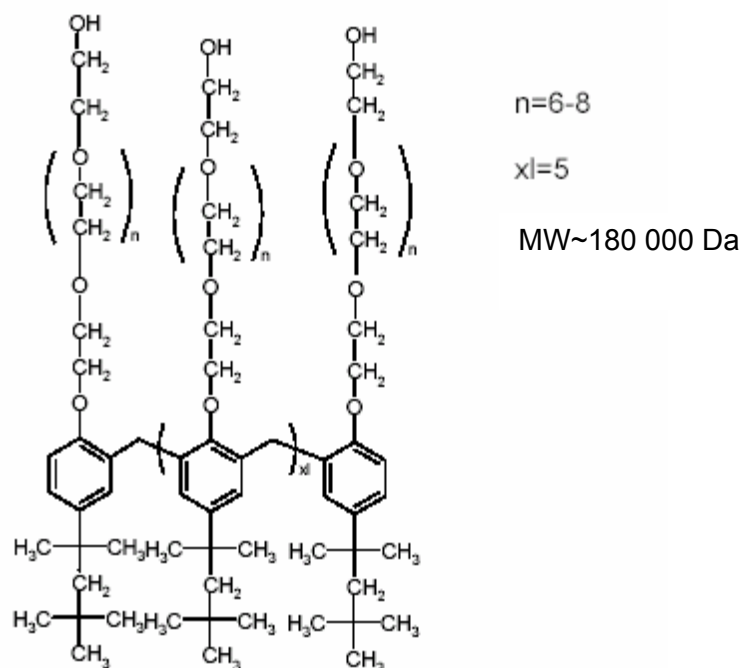


**Figure 3-4: Chemical structure of Tyloxapol®**

#### 3.1.4.2 Poloxamer 188

Poloxamer 188 is a white or almost white waxy powder, microbeads or flakes with a melting point around 50 °C. As all poloxamers, it is very soluble in water and alcohol (Sweetman 2004). Chemically, poloxamer consist of a synthetic block copolymer of  $\alpha$ -Hydro- $\omega$ -hydroxypoly (oxyethylene) poly (oxypropylene) poly (oxyethylene) with the general formula shown in Figure 3-5.

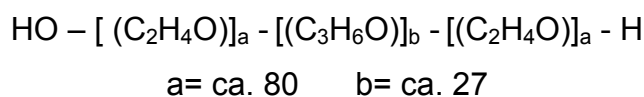


**Figure 3-5: Molecular formula of Poloxamer 188**

It has an average molecular weight from 7680 to 9510. Poloxamer 188 has an HLB value of 29 (American Pharmaceutical Association 1994). Poloxamer 188 was ordered as Lutrol®F68 from BASF AG (Ludwigshafen, Germany).

#### 3.1.4.3 Polyvinyl alcohol

Polyvinyl alcohol (PVA) is obtained by polymerisation of vinyl acetate followed by partial or complete hydrolysis in presence of catalytic amounts of alkali or mineral acids. Granules or powder are white to cream-coloured and odourless (Sweetman 2004). The PVA used in this work was purchased from Fluka (Buchs, Switzerland)

with the name Mowiol<sup>®</sup> 4-88 (The number 4 refers to the viscosity of a 4 % aqueous solution in mPa·s; the number 88 represents the percentage of hydrolysis). The product is a polymer with a molecular weight of ~31 000. The chemical formula of the polymer can be seen in Figure 3-6, where  $n \sim 630$  for the product used in the present work.

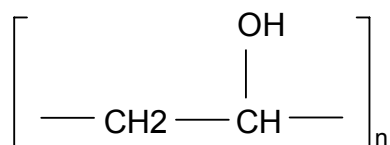


**Figure 3-6: Molecular formula of Polyvinyl Alcohol**

Its functionality as pharmaceutical excipient is mainly as coating agent, non-ionic surfactant and viscosity-increasing agent. It is soluble in water, but due to partial hydrolyzation of the vinyl acetate polymer, it is not soluble in cold water. An effective dissolution of the polymer requires the dispersion and continued mixing of the solid in cold or tepid water followed by sustained heating at 85-95°C until dissolved (American Pharmaceutical Association 1994).

#### 3.1.4.4 Purified soy lecithin

Lecithin is a non-synthetic emulsifying agent which can be totally biodegradable and metabolized, since it is part of biological membranes. A very important fact for the use of lecithin in inhalation is that dipalmitoylphosphatidylcholine (DPPC) conforms the 70-80 % of the lipids present in the natural lung surfactant (consisting in 80-90 % lipids) (McAllister, Alpar et al. 1996). This may reduce the risk of toxicity in pulmonary formulations which are often planned for repetitive administration. Additionally, the surfactant possesses a GRAS status conferred by the FDA. The Figure 3-7 shows the chemical structure of the amphoteric molecule of phosphatidylcholine. Purified soy phosphatidylcholine Phospholipon<sup>®</sup> 90G Phospholipon<sup>®</sup> 80 were a kind donation from the company Phospholipon GmbH (Cologne, Germany). Phospholipon<sup>®</sup> 90G is a pale yellow to yellow granular material containing 92–98 % purified phosphatidylcholine. Phospholipon<sup>®</sup> 80 is a yellowish to brown solid containing around 76 % of phosphatidylcholine, including small amounts of impurities such as phosphatidylethanolamine, sphingomyelin, and hydrogenated lyso-phosphatidylcholine.

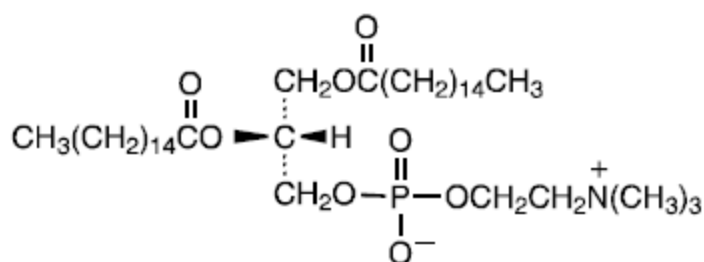


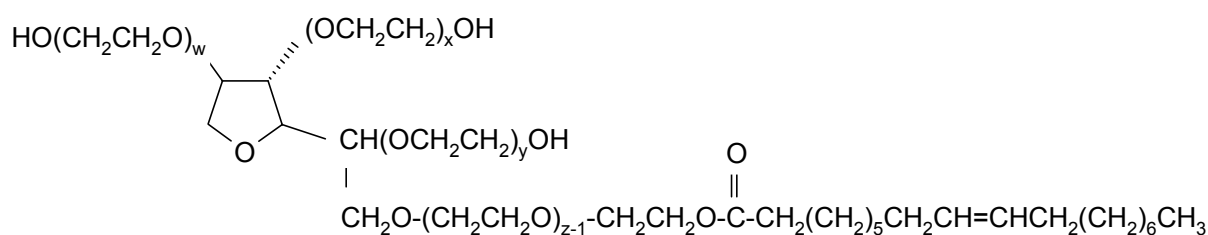
**Figure 3-7: Chemical structure of phosphatidylcholine**

#### 3.1.4.5 Sodium glycocholate

Sodium glycocholate is a built salt used here as an anionic surfactant in formulations stabilized with Phospholipon<sup>®</sup> 80 to supplement the steric stabilization with electrostatic stabilization. The product was purchased from Sigma-Aldrich (Deisenhofen, Germany).

#### 3.1.4.6 Tween<sup>®</sup> 80

Polysorbat 80 (Polyoxyethylen(20)sorbitan monooleate), Tween<sup>®</sup> 80 V Pharma was received from the company Uniqema (ICI Surfactants, Eversberg, Belgium). Its HLB value is 15. It is a non-ionic surfactant with a relatively low toxicity. For example for pulmonary application, the product Pulmicort Respules<sup>®</sup> budesonide inhalation suspension (Astra Zeneca 2002) contains this surfactant. The Figure 3-8 represents the structure of the molecule.



$$\text{Sum of } w + x + y + z = 20$$

**Figure 3-8: Chemical structure of Tween<sup>®</sup> 80**

### 3.1.5 Other materials

#### 3.1.5.1 Polyvinyl pyrrolidone

Although polyvinyl pyrrolidone (PVP) has well known properties as emulsifying agent, it was used in this work as carrier polymer in the preparation of solid dispersions of BPQ. In the formulation of solid dispersions with poorly water soluble drugs, PVP prevents or delays the dissolved portion of the active substance from crystallizing out by forming soluble complexes with it. Increasing the amorphous component can lead in many cases to an enhancement of dissolution rate of lipophilic active substances (hydrophilization effect) and can improve the physical stability of the formulations. The chemical structure of PVP can be seen in Figure 3-9. It is a free flowing white or yellowish-white powder very soluble in water.

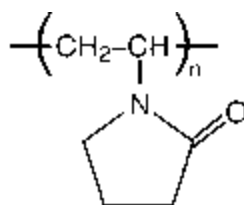


**Figure 3-9: Chemical structure of Polyvinyl pyrrolidone**

PVP K-30 was a gift from BUFA B.V. (Uitgeest, The Netherlands). The K value corresponds to the molecular weight of the product, which in this case is within the range 27.0 to 32.4 KDa, according to USP and Ph. Eur. specification.

#### 3.1.5.2 Inulin

Inulins are oligosaccharides produced by several plants, typically found in roots and rhizomes, for example in Chicory (*Cichorium intybus*) or onion (*Allium cepa*). Inulins are polymers mainly comprised of fructose units (2 to 140) joined by a beta-(2-1) glycosidic bond. At the end of the main fructose chain, there is a glucose unit, linked by an alpha(1-2) bond (Niness 1999). See Figure 3-10 for structure. Inulin is a white crystalline powder, used in this work as a drug carrier in the preparation of BPQ solid dispersions. The industrial process yielding the crystalline  $\alpha$ -modification of inulin, results in a product which is not soluble in cold water, only in warm water. An enzymatic step in the production of different types of inulins, will yield products with controlled degree of polymerization (DP). The compound has a GRAS status from

regulatory authorities. Inulin was chosen for the preparation of solid dispersions of BPQ, due to its non-toxicity and good stabilizing properties when interacting with lipophilic substances showed in previous work (Hinrichs, Prinsen et al. 2001; van Drooge, Hinrichs et al. 2004; van Drooge, Hinrichs et al. 2004). The inulin used was the inulin type TEX!803 (Inulin DP23), kindly provided by Sensus, (Roosendaal, The Netherlands).

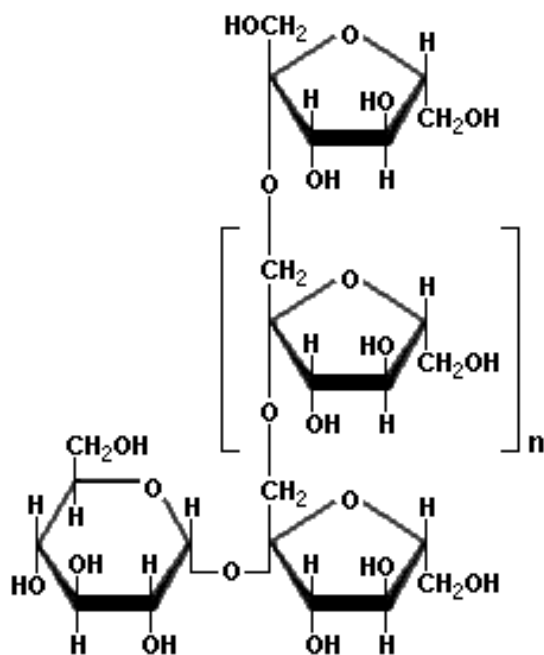


Figure 3-10: Chemical structure of inulin

### 3.1.5.3 Glycerol

Uncontrolled osmolarity in formulations delivered to the lung by means of aerosol or spray may induce cough or bronchospasm. Hypotonic and hypertonic nebuliser formulations produce bronchoconstriction through a combination of mast cell and reflex-mediated mechanisms (Beasley, Rafferty et al. 1988). In order to avoid that, glycerol (1,2,3-propantriol) was used as tonicity agent to control the iso-osmolarity of the formulations ( $\sim 250$ - $330$  mOsm/Kg). Glycerol 85% Ph. Eur. was purchased from the company Aug. Hedinger GmbH (Stuttgart, Germany). Glycerol has a GRAS status and has been reported before in nebulizer formulations proposed for inhalation available in the market (e.g. Tacholiquin<sup>®</sup> (bene Arzneimittel GmbH 1995)).

#### **3.1.5.4 Water**

For all formulations, Milli Q plus water (Millipore/Schwalbach, Germany), purified by reverse osmosis was used.

#### **3.1.5.5 Nebulizer systems**

In the inhalation of drugs by means of a nebulization system, the delivery system is not only conformed by the formulation itself, but also by the appropriate nebulizer which is capable to produce an aerosol with the required characteristics (e.g. Mass median aerodynamic diameter MMAD) that can achieve a defined area of deposition. Therefore, nebulizer systems used to test the performance of the different nanosuspensions prepared are described here, not as part of the formulation, but as part of the delivery system. The nebulizers selected for this work, as well as their characteristics of performance provided by the manufacturer (based on the nebulization of saline solution) are summarized in the Table 3-1.

**Table 3-1: Nebulization systems used to test nanosuspensions**

Nebulizers		
Nebulizer model	Manufacturer	Characteristics
<b>JET NEBULIZERS</b>		
Pari Boy Turbo system Pari LC Plus Turbo + Pari Boy compressor	Pari GmbH (Starnberg, Germany)	- Jet flow: 3-6 L/min - Output 500 mg/min - Operating pressure: 0.5 – 2 bar - MMD ~ 3.5 $\mu\text{m}^*$ - Fraction < 5 $\mu\text{m}$ 68 %
Pari LC Star nebulizer + Pari Boy compressor	Pari GmbH (Starnberg, Germany)	- Jet flow: 2-6 L/min - Output 450 mg/min - Operating pressure: 0.5 – 2 bar - MMD ~ 2.8 $\mu\text{m}^*$ - Fraction < 5 $\mu\text{m}$ 89 %
Respi-jet Kendall	Tyco Healthcare Deutschland GmbH (Germany)	- Jet flow: 4-6 L/min - Output 511 mg/min - Operating pressure: 1.25 bar - MMD ~ 3.45 $\mu\text{m}$
<b>ULTRASONIC NEBULIZER</b>		
Multisonic	Otto Schill GmbH & Co. KG (Probstzella, Germany)	-Operation frequency: 1.7 mHz -Nebulization rate: 0.75 mL/min -MMD ~ 4.7 $\mu\text{m}$
<b>PASSIVE VIBRATING MESH ULTRASONIC NEBULIZER</b>		
Omron U1	Omron Healthcare Europe B.V. (Hoofddorp, The Netherlands)	-Ceramic mesh pore size: 4.6 $\mu\text{m}$ -Operation frequency: 65 kHz -Nebulization rate: 0.25 mL/min -MMD ~ 7 $\mu\text{m}$

\*MMD measured with Malvern MasterSizer X at 23°C, 50% relative humidity and inspiratory flow of 20 L/min.

## 3.2 Methods

If no other information is given, the following methodology was performed at the Department of Pharmaceutical Technology, Biotechnology and Quality Management of the Freie Universität Berlin.

### 3.2.1 Production of nanosuspensions with high pressure homogenisation

#### 3.2.1.1 Operation principle of a piston-gap type high pressure homogeniser

Aqueous BPQ nanosuspensions were prepared by high pressure homogenisation according to the technique described by Müller and collaborators in 1994 (Müller, Becker et al. 1994; Müller, Becker et al. 1999). Samples of 20-40 mL volume were obtained with a piston-gap type APV Gaulin Micron LAB 40 (APV Systems, Unna, Germany) homogenizer, discontinuous version. The operative homogenisation pressure for this model is in the range 100-1500 bar. Combined mechanisms of cavitation, turbulence and crystal collision are responsible of the particle size reduction of the drug crystals. The operation principle is based in the *Bernoulli equation* which establishes that the sum of static pressure in the flow plus the dynamic pressure is equal to a constant throughout the flow (total pressure of the flow):

$$P_s + \frac{\rho V^2}{2} = K$$

where:

$P_s$  = static pressure

$\rho$  = density

$V$  = velocity

$K$  = Constant pressure of the flow

$\frac{\rho V^2}{2}$  = Dynamic pressure

During the process, the suspension is contained in a 3 cm diameter cylinder and it will narrow when entering in the homogenisation gap (3  $\mu\text{m}$ ). This will produce that the streaming velocity and therefore the dynamic pressure in the homogenisation gap

dramatically increases. Simultaneously, the static pressure decreases and falls below the vapour pressure of the dispersion medium (normally water) at room temperature. This leads to the boiling of water at room temperature, formation of gas bubbles, which implode when the liquid leaves the gap and the pressure suffers an abrupt increase (=cavitation). The implosion of the gas bubbles cause shock waves which originate the diminution of particles (crystals). It is nowadays understood that the formation of bubbles and the turbulences resulting of them (i.e. shear forces) are a decisive factor for the reduction in particle size. Collision of the particles at high speed breaks them into nanoparticles (Müller and Böhm 1998).

### 3.2.1.2 Preparation of Nanosuspensions

A critical parameter that defines the quality of nanosuspensions is the homogeneity of the nanocrystals size. That means the narrowing of the size distribution of the nanocrystals population. The Ostwald ripening effect occurs due to different saturation solubilities in the vicinity of differently sized particles. The presence of a concentration gradient in the solution around small (nm) and larger particles ( $\mu\text{m}$ ) will induce compensation of such a gradient, resulting in the dissolution of smaller particles and crystal growth due to precipitation of the drug in the supersaturate vicinity of the larger particles. The homogenisation process is able to narrow the size distribution depending mainly on the crystal hardness of the drug, the applied homogenisation pressure and the applied number of homogenisation cycles.

In order to develop a nanosuspension formulation a screening using different aqueous dispersion media was performed. Different surfactant solutions will yield specific stability with the same drug molecule due to differences in adsorption onto the surface of the drug particles during the homogenisation process. Furthermore, the viscosity and concentration of the surfactant at the production temperature will also directly influence the long-term stability and quality of the formulation.

To prepare the nanosuspensions for screening, as well as those used for the *in vitro* and *in vivo* tests designed for the pulmonary delivery of BPQ, the manufacture protocol was:

1. The drug powder was pre-dispersed in aqueous surfactant solution by means of mortar and pestle.
2. The coarse powder was dispersed for one minute by using an Ultra-turrax T25 (Janke und Kunkel GmbH, Staufen, Germany) at 8000 rpm.

3. The dispersion was then pre-homogenized using the high pressure homogeniser running 2 cycles at 150 bar followed by 2 more cycles at 500 bar.

4. 40 cycles at 1500 bar were used to complete the homogenisation process, resulting in the homogenisation time at which the maximum power density was reached at this homogenisation pressure with a homogenisation gap  $\sim 3 \mu\text{m}$  width.

The drug content in most of the cases was 1%, and concentrations up to 7 % were investigated in selected cases.

Due to application of energy during the homogenisation process at 1500 bar, the product can increase the temperature by 15 to 20 °C. After several cycles this increment might affect the quality of the product. Therefore, for the production of BPQ nanosuspensions, the temperature of the suspension was cooled down after each cycle to a room temperature range from 21-23 °C in order to have a controlled production at room temperature.

The nanosuspensions were adjusted to iso-osmolarity by addition of glycerol to the formulation (see section 3.1.5.3). Osmolarity was controlled by means of a cryoscopic osmometer Osmomat 030 (Gonotec GmbH, Berlin Germany).

## **3.2.2 Characterization of drug nanosuspensions: size distribution, crystal nature and zeta potential**

### **3.2.2.1 Laser Diffraction (LD)**

The laser diffraction technique is based on the phenomenon that particles scatter light in all directions with an intensity Fraunhofer diffraction pattern that is dependent on the particle size. Simplified, the diffraction angle is small for the large particles, as their surfaces are less curved, while for small particles with a more curved surface, the diffraction angle is larger. The Figure 3-11 shows the simplified principle of operation of a laser diffractometer.

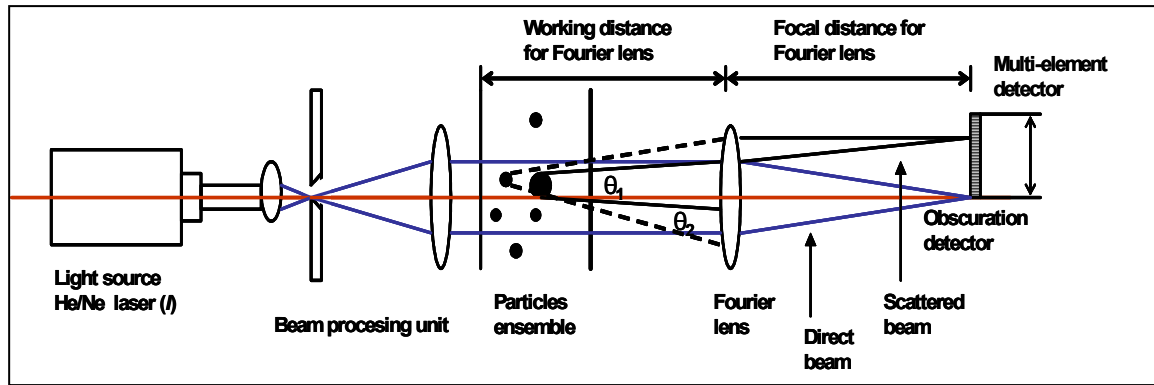


**Figure 3-11: Representation of the set-up of a laser diffraction instrument.**  
Adapted from the international standard ISO 13320-1 (Technical Committee LBI/37 2000).

All present instruments assume a spherical shape for the particles. The laser diffraction technique cannot distinguish between scattering by single particles and scattering by clusters of primary particles forming agglomerates or aggregates. In the present work the instrument Coulter<sup>®</sup> LS 230 (Beckmann- Coulter Electronics, Krefeld, Germany) was used. As light source it works with a laser wavelength of 750 nm. An optical system conducts the laser beam towards the particles ensemble, where it will enter the particle to be absorbed or refracted. At a certain distance, a Fourier lens reproduces the image of the particles independently of their position in the measuring cell always in the same ring of the multi-element detector. The intensity of the diffraction pattern increases with the number of diffracting particles. This pattern can be mathematically resolved to yield a volume distribution of the particles. The volume distribution can be calculated applying the Fraunhofer theory or the Mie theory, depending on the characteristics of the sample. Historically, instruments only used scattering angles smaller than  $14^\circ$ , which limited the application to a lower minimal size of about  $1 \mu\text{m}$ . The reason for this limitation is that smaller particles show most of their distinctive scattering at larger angles. Many recent instruments (as the one used in this work), allow measurement at larger scattering angles, typically from 60 to 146 degrees, allowing the measurement of particles down to about  $0.04 \mu\text{m}$  and up to  $2000 \mu\text{m}$ . This was possible due to the Polarization Intensity Differential Scattering-technology (PIDS) that complements the detection system, which allow with high resolution determination of particles below  $1 \mu\text{m}$ . In this PIDS technology, a light beam (of intensity  $I$ ) with several wavelengths (from typically a tungsten-halogen lamp) is polarized in either vertical (V) or horizontal (H) directions, passing the

sample. The detected scattering intensity  $I_V$  and  $I_H$  at a given angle will be different. The difference between both ( $I_V - I_H$ ) is termed the PIDS signal. The scattered light is detected by detectors located at a wide angular range (60-146 degrees) (Xu 1997). In general terms, for the data analysis of particles  $\geq 4 \mu\text{m}$ , the Fraunhofer theory is applicable (Washington 1992). For particles smaller than  $4 \mu\text{m}$ , or more precisely smaller than 4 times the wavelength of the light used for generating the diffraction pattern, the Mie theory should be used for calculations. However, in contrast to the Fraunhofer theory, the Mie model takes into account the real and the imaginary refraction index of the particles. The real part corresponds to the refraction properties and the imaginary part represents the absorption. The refractive index of a completely transparent material would consist of only a real part, and the imaginary part would be zero. Alternatively, a coloured material would have a refractive index with both a real part and an imaginary part. For the yellow coloured drug BPQ, the real refraction index was measured 1.456 and the imaginary part is 0.01 (Keck 2006). These values were introduced in a specific optical model for the calculation of the particle size using the software Beckmann Coulter- Particle characterization version 3.19. The refraction index of the dispersion medium used was 1.332, which corresponds to distilled water, where the nanocrystals were measured. LD data were evaluated using the volume distribution diameters  $d_{50\%}$ ,  $d_{90\%}$ ,  $d_{95\%}$  and  $d_{99\%}$ . For example, a diameter 50% ( $d_{50\%}$ ) value of  $1 \mu\text{m}$  indicates that 50% of the particles possess a diameter below  $1 \mu\text{m}$ . Each sample was measured three times consecutively.

### 3.2.2.2 Photon Correlation Spectroscopy (PCS)

PCS or dynamic light scattering analyses scattered laser light from particles diffusing in a low viscosity dispersion medium (e. g. water). The detected intensity signals (photons) are used to calculate the correlation function, from the decay of this correlation function the diffusion coefficient  $D$  of the particles is obtained. Applying the Stokes-Einstein equation:

$$r = \frac{kt}{6\pi\eta D}$$

where:

$r$  = hydrodynamic particle radius

$k$  = Boltzmann's constant

$t$  = absolute temperature

$\eta$  = dynamic viscosity of the dispersion medium

$D$  = Diffusion constant ( $\text{cm}^2/\text{s}$ )

the radius of the particles can be calculated.

The fluctuations in the intensity of the scattered light, originated from the random diffusion of the particles, are measured. Small particles will diffuse faster and fluctuations of the scattered light are therefore relatively more rapid. The mean particle size diameter can be calculated (Z-average). In addition a polydispersity index (PI) is obtained as a measure for the width of the distribution. The PI is 0 in case a monodisperse particle population is present. PI values of around 0.10 – 0.20 indicate a relatively narrow distribution, values of 0.5 and higher are obtained in case of very broad distributions. The measuring range of PCS is approximately 3 nm – 3  $\mu\text{m}$ .

A PCS apparatus consists of a laser, a temperature controlled measuring cell and a photomultiplier for detection of the light scattered at a certain angle. The signal originated in the photomultiplier is transferred to a correlator for the calculation of the correlation function  $g(\tau)$ . This calculates the diffusion coefficient of the particles and the respective particle size. In this work, a Zetasizer 4 (Malvern Instruments, Malvern, UK) was used to measure the BPQ nanocrystals. The instrument was equipped with a laser beam ( $\lambda=633$  nm), an angle of  $90^\circ$  was used for signal detection by a photomultiplier. Samples were diluted in distilled water to an appropriate concentration and measured in triplicate.

### **3.2.2.3 Zeta potential and Laser Doppler Anemometry (LDA)**

Zeta potential is an important parameter in the assessment of the physical stability of colloidal dispersions. The zeta potential only exists when the surface of a particle is in contact with a liquid. When a particle is suspended in a liquid, ions of opposite charge from this liquid are attracted to the surface of the particle. In addition functional groups at the particle surface dissociate, creating the surface potential (=Nernst potential). The development of a net charge at the particle surface affects the distribution of ions in the surrounding interfacial region, resulting in an increased

concentration of counter ions (ions of opposite charge to that of the particle) close to the surface. Thus an electrical double layer exists around each particle. The liquid layer surrounding the particle exists as two parts; an inner region, called the Stern layer, where the ions are strongly bound and an outer, diffuse region where they are less firmly attached. Within the diffuse layer there is a notional boundary inside which the ions and particles form a stable entity. When a particle moves (e.g. due to gravity or an electric field), ions within the boundary move with it, but any ions beyond the boundary do not travel with the particle. This boundary is called the surface of hydrodynamic shear or slipping plane. The potential that exists at this boundary is known as the zeta potential  $\zeta$  (Müller 1996; Malvern Instruments 2004). The zeta potential can be understood as a remote effect of the surface charge affecting the interactions between charged particles and influencing the stability of a colloidal system.

By means of the Laser Doppler Anemometry (LDA) the velocity of the particles in dispersion media can be detected from the scattered light. Light scattered from particles in movement experiences a frequency shift, known as Doppler effect. To detect this high frequency shift, two laser beams derived from the same source and with the same path length are arranged to cross. The resulting frequency spectra measured are then transferred to electrophoretic mobilities (particle velocity), and subsequently converted to a zeta potential by means of the Helmholtz-Smoluchowski equation (Malvern Instruments 1998). Samples were measured in triplicate using a Zetasizer 4 (Malvern Instruments, Malvern UK). As dispersion medium bidistilled water adjusted to a conductivity of 50  $\mu\text{S}/\text{cm}$  (Müller 1996) with NaCl isotonic solution was used, the pH was controlled between 6.0 and 7.0.

#### **3.2.2.4 Polarized light microscopy**

A polarizing light microscope equipped with a linear polarizer was used to obtain a general overview of the drug nanocrystals in terms of crystal size and presence of crystal aggregates. The detection of a small population of microcrystals content in a nanosuspension is sometimes not possible using LD technique. If detectable, microparticles could consist of aggregates of small nanocrystals rather than microcrystals, especially in poorly stable nanosuspensions. Therefore, samples were analyzed using a light microscope Orthoplan Leiz (Wetzler, Germany) at a 1000 $\times$  magnification with immersion oil. The microscope was attached to a camera CF20DX

(Kappa). The use of polarised light enables the imaging of nanoparticles in the range between 200-300 nm as the lower limit of detection.

### 3.2.2.5 X-Ray Diffraction

The method was used in order to characterize the crystalline state of the nanosuspensions prepared. Random arrangement of molecules in noncrystalline substances makes them to poor coherent scatterers of X-rays, resulting in broad, diffuse maxima in diffraction patterns. Their X-ray patterns are easy to distinguish from crystalline forms, which show sharply defined diffraction peaks. X-ray diffraction methods analyze the pattern of scattered X-rays by causing a beam of monochromatic X-rays to impinge on a crystal and measure the intensity (the amplitude of the scattered beam) variation of the scattered x-rays around the crystal. The directions of the diffracted beams are related to the shape and dimensions of the unit cell of the crystalline lattice. The diffraction intensity depends on the disposition of the atoms within the unit cell. The Braggs law describes this phenomenon. It states that diffraction can occur only when waves that are scattered from different regions of the crystal, in a specific direction, travel distances differing by integral numbers ( $n$ ) of the wavelength ( $\lambda$ ). Under those conditions, the waves are in phase. The Braggs law is described by the following equation:

$$\frac{n\lambda}{2 \sin \theta} = d_{hkl}$$

where  $d_{hkl}$  represents the interplanar spacing for a specific set of parallel planes  $hkl$  in the crystal and  $\theta$  is the angle of diffraction (United States Pharmacopeial Convention Inc. 2006).

X-ray diffraction studies were conducted with an STOE STADI P. diffractometer (Stoe & Cie GmbH, Darmstadt, Germany) equipped with a  $6^\circ$  position sensitive detector (PSD) and setup in Debye-Scherrer geometry. The X-ray source was a 1500W sealed tube with a Cu target used with a Ge (111) monochromator to give Cu  $K\alpha_1$  radiation (Wavelength = 1.5406 Å). The sample holder was rotated about the axis to increase the number of crystallites in differing orientations contributing to the sample pattern, thus obtaining a better diffraction pattern. The aqueous dispersion was measured in colloidal state, directly in the system by means of a capillary sample holder. X-ray measurements have been performed in collaboration with Mr. Klaus-J. Wenzel at the *Federal Institute for Materials Research and Testing (BAM)*.

### 3.2.2.6 Scanning Electron Microscopy (SEM)

This technique was used in this work to investigate the shape and surface morphology of the drug nanocrystals and to assess the particle size.

Aqueous dispersions of drug nanocrystals were dropped and spread on a sample holder with double sided tape and coated under an argon atmosphere with gold to a thickness of 6.5 nm (SCD 040, Balt-Tec GmbH, Witten, Germany) in order to increase sample conductivity. The samples were placed inside of the microscope's vacuum column and the air was pumped out. An electron gun situated at the top of the column emits a beam of high energy electrons (primary electrons). This beam passes through the lenses which concentrates the electrons to a very fine spot and scan across the specimen row by row. As the focused electron beam hits each spot on the sample, secondary electrons are emitted by the specimen through ionization. A detector counts these secondary electrons. The electrons are collected by a laterally placed collector and these signals are sent to an amplifier. Nanocrystals have been observed with a scanning electron microscope S-4000 (Hitachi High-Technologies Europe GmbH, Krefeld, Germany) using secondary electron imaging at 10 keV. SEM uses series of glass lenses to bend electrons and create a magnified image. SEM studies have been performed together with Mr. Gernert at the *Zentraleinrichtung Elektronenmikroskopie (Technische Universität Berlin, Germany)*.

### 3.2.2.7 Viscosity and density

The viscosity of the nanosuspensions was measured using an Ubbelohde-type viscometer AVS 350 (Schott-Geräte GmbH, Mainz, Germany) (European Pharmacopeia 1997; United States Pharmacopeial Convention Inc. 2006). About 15 mL of sample were introduced using a pipette long enough to prevent wetting the sides of the tube. Flow through the capillary occurs under the influence of gravity. The capillary was then clamped vertically in a water bath at a constant temperature of  $25 \pm 0.1$  °C and allowed to attain the required temperature (10 min). The method was adjusted so that the flow time for all formulation was within the range 100-150 sec.

The corrected flow time  $t$  was then multiplied by the viscometer constant  $c$  resulting in the kinematic viscosity [ $\text{mm}^2/\text{s}$ ] or [cSt]) directly.

$$v = ct$$

The viscometer constant  $c$  is mentioned in the enclosed production certificate and was equal to 0.009447 for the capillary used.

In this work, the dynamic viscosity ( $\eta$ ) rather than the kinematic viscosity ( $\nu$ ) was used to characterize the nanosuspension. The dynamic viscosity was calculated from the formula:

$$\eta = \nu\rho$$

where  $\rho$  corresponds to the density of the fluid, which was measured using a Density meter DMA 38 (Anton Paar GmbH, Graz, Austria). Values were reported in mPa·s. Measurements were performed in triplicate.

### **3.2.2.8 Surface tension**

In order to determine the surface tension of the nanosuspensions, the Wilhelmy plate method was used. The test was performed with a platinum plate attached to a Tensiometer K10 (Krüss, Hamburg, Germany). The measurements were done at a constant temperature of  $25 \pm 0.1$  °C and reported in mN/m.

### **3.2.2.9 In vitro dissolution tests for nanosuspensions**

The dissolution of buparvaquone nanocrystals produced with different particle sizes were tested to evaluate improvement in the dissolution rate of the crystals present in the formulation, related to the original crystalline powder. In order to meet sink conditions, the dissolution medium consisted of a 2% polyoxyethylenesorbitan monolaurate (Tween 80) solution prepared with demineralised water. The pH of the dissolution medium was approximately neutral. One millilitre of nanosuspension was discharged with a pipette at the bottom of the vessel containing 500 mL of dissolution medium. In the case of the original crystalline powder, 10 mg of the powder were set inside of the baskets included in the apparatus. All dissolution tests were performed using the paddle method, on a USP dissolution apparatus I (Rowa Techniek B.V., Leiderdorp, The Netherlands) at 50 rpm. Measurements were done in triplicate. BPQ concentration per vessel was measured every 2 min spectrophotometrically at 288 nm (Pharmacia LKB-Ultrospec III, Uppsala, Sweden). The wavelength was selected determining the UV spectra (200-400 nm) of the drug solution in the dissolution media and matching it against that obtained for the dissolution media alone. The detector was calibrated preparing a calibration curve in the range from 0.01 to 10 mg/500 mL using the dissolution media to prepare the calibration standards and

using blank correction. The best-fit calibration line was determined each time by sum-squared linear regression analysis of the calibration data. The curve was done with seven concentration levels. The coefficient of correlation calculated for the method was  $r^2 = 0.9956$  within the calibration range (0.01-10 mg/500 mL). Dissolution tests were performed at the *Department of Pharmaceutical Technology and Biopharmacy, University of Groningen Institute for Drug Exploration (GUIDE)*.

#### **3.2.2.10 HPLC method to determine the content of buparvaquone**

To determine the content of BPQ in the nanosuspensions prepared and to follow up the stability of the drug molecule in the dispersions, an HPLC method was adapted. The same method was used to determine the saturation solubility of the nanosuspensions. The HPLC system used consisted of an autosampler model 560, a pump system model 525 and a diode array detector model 540 (Kontron Instruments, Germany). The system is linked to a KromaSystem 2000 v. 1.70 data acquisition and process system, which also controls the HPLC modules. The UV-spectrum of buparvaquone under the conditions of the method presents mainly two maximums of absorbance, one of higher intensity at 252 nm and the second at 281 nm. In this case, the detector was set at a wavelength of 252 nm.

Calibration samples were prepared by dissolving BPQ crystalline powder in a dissolution mixture of methanol-dimethylformamide (99:1 v/v). The calibration range from 10 to 100 µg/mL. 50 µL of the nanosuspension to be quantified were diluted to a volume of 10 mL with the same dissolution mixture. 200 µL of the tests and calibration samples were added with 50 µL of internal standard solution containing 100 µg/mL of parvaquone and diluted with 600 µL of mobile phase. 20 µL were injected onto a reverse phase column Hypersil SAS (5 µm) 250 x 4 mm i.d. eluted at 1 mL/min flow with a mobile phase composed of 0.05 M sodium acetate buffer (pH 3.6) and methanol (15:85 v/v) (Kinabo and Bogan 1988). Internal standard method was used for calculation, based on buparvaquone/parvaquone peak area ratio. As before, the best-fit calibration line was determined each time by sum-squared linear regression analysis of the calibration data using five different concentration levels. The coefficient of correlation calculated for the method was  $r^2 = 0.9932$  within the calibration range (1-100 µg/mL).

### 3.2.3 Methods used during the *in vitro* characterisation of aerosol produced during the nebulisation of nanosuspensions

Therapeutic aerosols require the control of physicochemical characteristics which directly affect the drug deposition in the respiratory system. From them, the aerosol droplet size distribution is probably the most important. Independently of the method used for this purpose, the aerosol needs to be immediately measured when leaving the mouth piece of the nebulizer, in order to avoid droplet coalescence. The measurements should be also performed under controlled inspiration flow and at constant conditions of temperature and relative humidity to control droplet evaporation. Aerosols produced by medical nebulisers are heterodisperse that is made up of particles of different sizes.

Most therapeutic aerosols conform to an approximately log normal distribution from which can be derived the mass median aerodynamic diameter (MMAD) and the geometric standard deviation (GSD). One problem is often seen when determining particle size, the use of MMAD and MMD as if they were interchangeable. MMD (mass median diameter) is measured by some light scattering devices and only describes the aerodynamic behavior of particles if they are spherical and of unit density (O' Callaghan and Barry 1997). The movement of the disperse phase in the aerosol depends on the size, shape and density of the droplets, properties which are combined in the term "aerodynamic diameter" ( $D_A$ ). For spherical particles with diameters  $> 0.5 \mu\text{m}$ , the relationship between the diameter and the aerodynamic diameter can be described by the following equation:

$$D_A = D \sqrt{\rho / \rho_0}$$

Where:

$\rho$  = density of the disperse phase

$\rho_0$  = Unit density ( $1\text{kg/dm}^3$ )

The same equation can be used to correlate the MMD and the MMAD. Therefore, for spherical aqueous droplets, MMAD equals MMD.

The two most commonly used method of aerosol particle size determination are laser based light scattering devices and inertial impaction devices (O' Callaghan and Barry 1997). It has been reported that both instrumentations are useful to describe the behavior of aerosol clouds produced by nebulisers, both have advantages and disadvantages which can yield non equivalent data (de Boer, Gjaltema et al. 2002).

### 3.2.3.1 Cascade Impaction Analysis

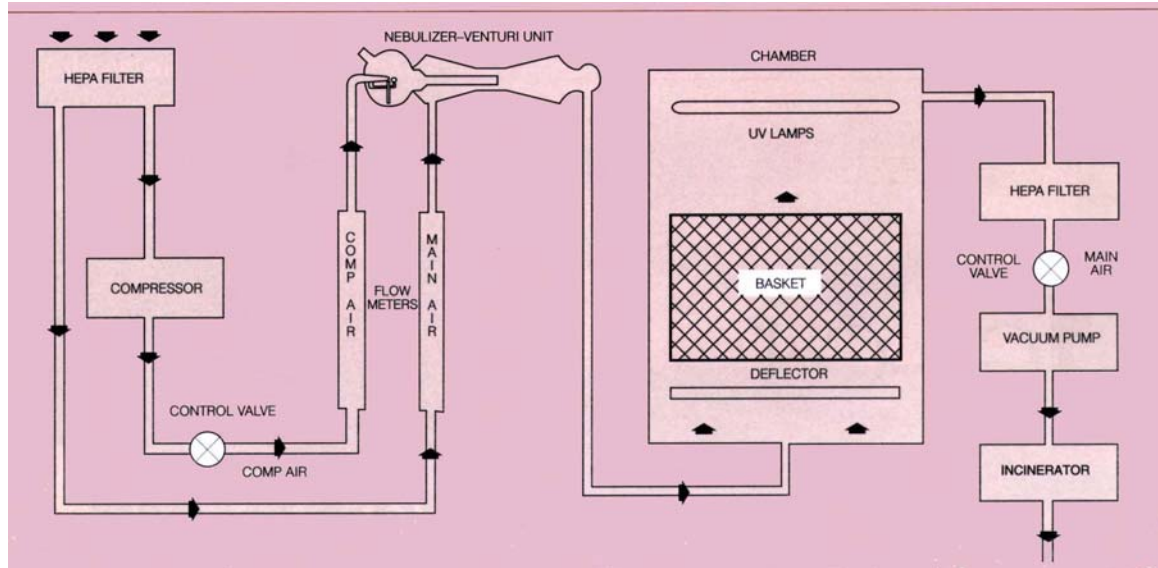
Compendial methods described in the British (British Pharmacopeia 1998), European (European Pharmacopeia 1997) and USP (United States Pharmacopeial Convention Inc. 2006) describe different impaction procedures to predict the behavior and characteristics of aerosol formulations. From all these methods, the Andersen cascade impactor is the most popular instrument for measuring respirable aerosols because it is inexpensive, relatively simple to operate, and provides direct and reproducible detailed measurement of aerodynamic mass distribution of a stable aerosol (Stapleton and Finlay 1998).

One important reason for using this inertial separation principle is that drug fractions are classified into aerodynamic size ranges that are relevant to the deposition in the respiratory tract. Measurement of these fractions with chemical detection methods enables establishment of the particle size distribution of the drug in the presence of excipients. However, the technique is laborious and time consuming and most of the devices used for inhaler evaluation lack sufficient possibilities for automation (de Boer, Gjaltema et al. 2002).

In this work, a whole body inhalation exposure chamber Glas-Col<sup>®</sup> Model A4224 (Glas-Col LLC, IN, USA) was used for the experimental inhalation therapy of *Pneumocystis* pneumonia infected mice. The system included a glass jet (venture) nebulizer into which the suspension was introduced. Pressurized air dispersed the formulation and the resulting aerosol was then drawn into the system by suction. The figure 3-12 represents this chamber.



(a)



(b)

Figure 3-12: (a) External view of the whole body inhalation chamber Glas-Col<sup>®</sup> Model A4224. (b) Diagram explaining the components and aerosol flow inside of the chamber (Glas-Col<sup>®</sup> 2000).

In order to characterize the aerosol distributed inside of this system, its MMAD and GSD were determined using an 8-stage Andersen Cascade Impactor (ACI-8, Thermo Electron, Franklin, MA, USA). The figure 3-13 shows the ACI-8.

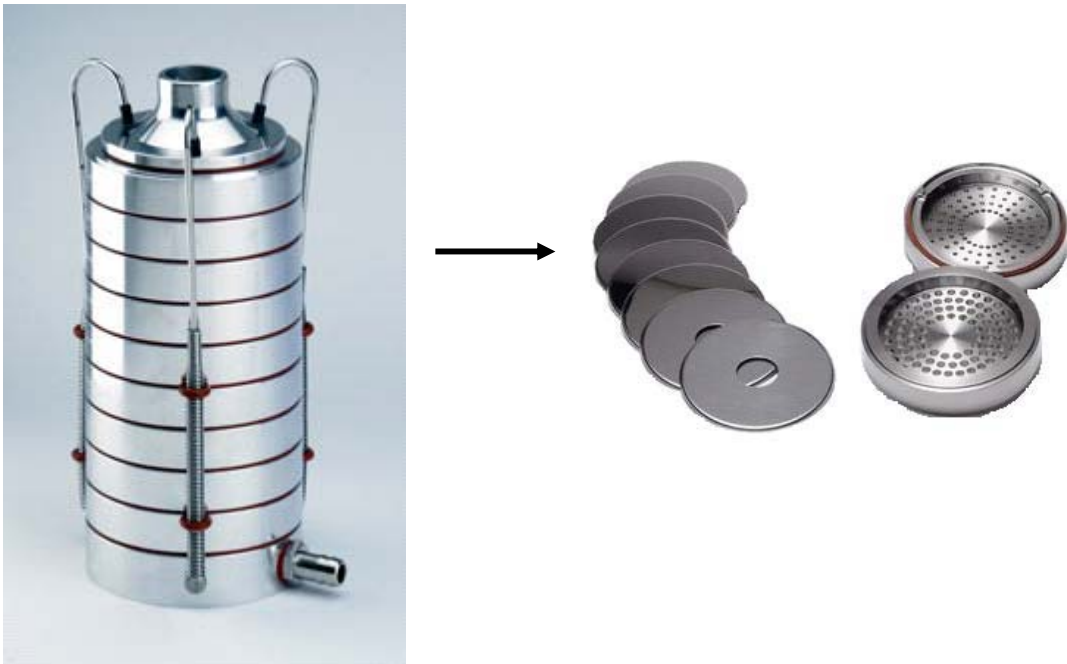


**Figure 3-13: Photograph of the assembled 8-stage Andersen Cascade Impactor (ACI-8). On the right side, a view of the individual components: separation stages and collection plates.**

The device was operated at a constant flow rate of 28.3 L/min, which had been calibrated by means of a rotameter. At this flow, the particle fractionation range is between 0.4 and 10  $\mu\text{m}$ . The eight stages correspond approximately to the various parts of the respiratory system as follows (Thermo Electron Corporation 2003):

- Stage 0: 9.0 - 10.0 microns
- Stage 1: 5.8 - 9.0 microns
- Stage 2: 4.7 - 5.8 microns (pharynx)
- Stage 3: 3.3 - 4.7 microns (trachea & primary bronchi)
- Stage 4: 2.1 - 3.3 microns (secondary bronchi)
- Stage 5: 1.1 - 2.1 microns (terminal bronchi)
- Stage 6: 0.7 - 1.1 microns (alveoli)
- Stage 7: 0.4 - 0.7 microns (alveoli)

The mass of drug deposited at each stage was recovered and analyzed by ultraviolet spectroscopy ( $\lambda = 252$  nm; DU640B Spectrophotometer, Beckman Coulter, Fullerton, CA, USA). The MMAD was calculated from the cumulative size distribution of the drug impacted on the different stages of the ACI. The GSD describes the spread of the particle size distribution and was also calculated according to the USP Pharmacopoeia (United States Pharmacopoeial Convention Inc. 2006). The calculation of the percent mass emitted by this jet nebulizer loaded with a specific BPQ formulation was determined according to the formula (Newman, Pellow et al. 1985):

$$\% \text{ mass} = \frac{\text{mass of drug added to the nebulizer} - \text{mass remaining in the nebulizer after nebulisation}}{\text{mass of drug added to the nebulizer}} \times 100$$

The nebulizer was operated until the dryness and the drug remaining in the device was quantified ( $n = 6$  measurements) by UV-spectrophotometry using a DU640B Spectrophotometer Beckman Coulter ( $\lambda=252$  nm). For the quantification of BPQ, as usual, the best-fit calibration line was determined each time by sum-squared linear regression analysis of the calibration data using seven different concentration levels. The coefficient of correlation calculated for the method was  $r^2 = 0.9997$  within the calibration range (0.4-40  $\mu\text{g/mL}$ ).

### 3.2.3.2 Laser diffraction analysis

For all the nanosuspensions tested, the aerosol size distribution during in vitro tests performed with different nebulization systems, the laser diffraction technique was used. In a first set of experiments, performed with two different formulations and 4 different type of nebulizers (see Table 3-1, page 49), 5 ml of each nanosuspension were nebulized during 5 minutes per device. Droplet size measurements of the VMD  $X_{50}$  (volume median diameter) were performed immediately after starting the nebulization process, in the middle (after 2.5 min) and at the end of the process (after 5 min). The system used in this study was a HELOS laser diffractometer with sprayer module (Sympatec, Clausthal-Zellerfeld, Germany). Measurements were performed applying the method previously described by Steckel and Eskandar developed for this specific instrument, using a 20 mm lens in the laser diffractometer (measuring range 0.18 to 35  $\mu\text{m}$ ) and a distance of 63 mm between the nebulizer and the focus of the lens (Steckel and Eskandar 2003). The ambient conditions during the

measurements were temperature  $25 \pm 1^\circ\text{C}$  and a relative humidity of  $50 \pm 5\%$ . Standard conditions were kept throughout the experiments in order to ensure a constant influence of these parameters in the measurements regarding evaporation and condensation of solvent water on the surface of the droplets. During the measurements of aerosol droplet size, a suction pump ( $\sim 20\text{L}/\text{min}$ ) was connected to remove the aerosol from the atmosphere and to avoid re-entering of the particles to the path of the laser beam. The distance between the measuring area and the suction pump was set ensuring that the vacuum flow did not affect the nebulization flow. The Figure 3-14 shows a representation of the system.

The parameters considered to characterize the aerosol droplets produced by the four selected nebulizers with the two buparvaquone formulations and the reference solutions (original dispersion media) in study, included the mass median diameter (MMD) calculated from the VMD  $X_{50}$  assuming spherical unit density particles, the percentage of aerosol droplets under  $5 \mu\text{m}$ , to evaluate the potential quantity of droplets that can actually reach the lungs, and the span value which was calculated using the known formula (McCallion et al. 1995):

$$\text{Span} = (90\% \text{ undersize} - 10\% \text{ undersize}) / 50\% \text{ undersize}$$

The main idea of this first set of experiments, was the comparisons of the aerosol droplet size distribution values (MMD and span) between two different BPQ nanosuspensions rather than the comparison between commercial nebulizers. In this first set of experiments the influence of the nebulizer technology on the particle aggregation of the drug nanocrystals (see 3.2.3.3) was also assessed. These studies were performed in the *Department of Pharmaceutical Technology of the Christian Albrechts Universität zu Kiel*.

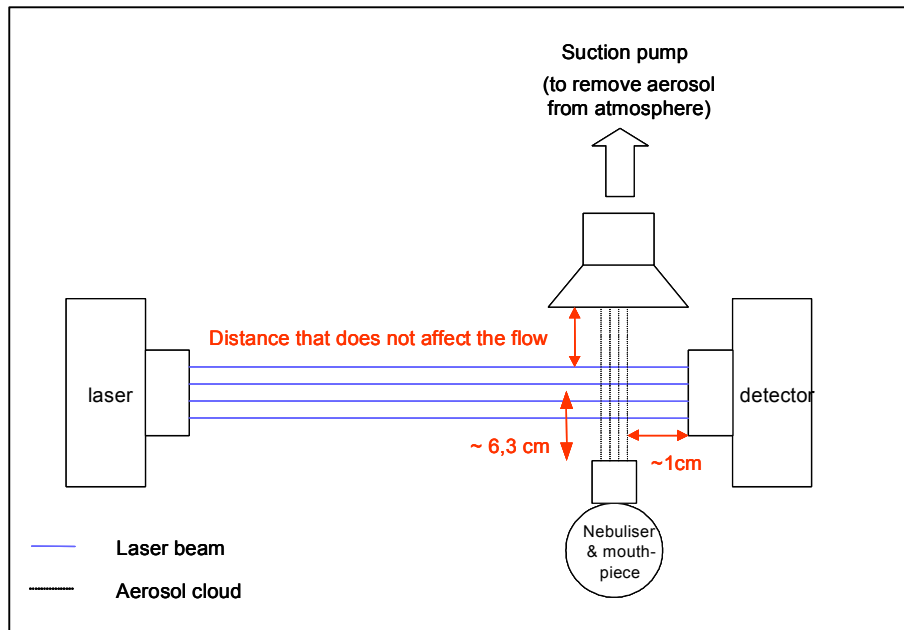


**Figure 3-14: Representation of the set-up of a laser diffraction instrument to measure droplet size of the aerosolized nanosuspensions. Modified after (Silkstone 1999; Mitchell, Nagel et al. 2003).**

In a second set of experiments, seven different stable formulations, with different physicochemical properties (viscosity, surface tension) and some of them with higher drug content were tested with one nebulizer device. The purpose was to investigate the influence of the excipients and drug concentration on the quality parameters of the droplets produced. For this second set of experiments, a more specific nebulizer for the deposition of particles in the deep peripheral area of the lungs, the Pari LC Star nebulizer attached to a Pari-boy compressor was used. 5 mL of each buparvaquone nanosuspension formulation was placed in the nebuliser reservoir. This system was connected to a laser diffraction apparatus Sympatec Helos BF/Magic<sup>®</sup>, equipped with a modular inhaler adapter (INHALER<sup>®</sup>2000) (Sympatec GmbH, Clausthal-Zellerfeld, Germany), and 100 mm lens. The Figure 3-15 shows the set up system used for the measurements. Calculations were made on the basis of the Fraunhofer theory. A constant inhalation flow 40 L/min was adjusted through the nebuliser. The measurement was started after a continuous aerosol output rate was established (after approximately 3 seconds from the start of the nebulization); each measurement lasted 10 seconds. Details about the functionality of the specific module can be found somewhere else (de Boer, Gjaltema et al. 2002). In this second set of experiments, the efficiency of the nebulization process for each formulation was not only evaluated in terms of particle size distribution (MMD, Span), but also the quantity of drug emitted by the nebulizer was studied (see 3.2.3.4), apart from the drug nanocrytal aggregation induced by the nebulization process (see 3.2.3.3). These studies were performed at the *Department of Pharmaceutical Technology and Biopharmacy, University of Groningen Institute for Drug Exploration (GUIDE)*.

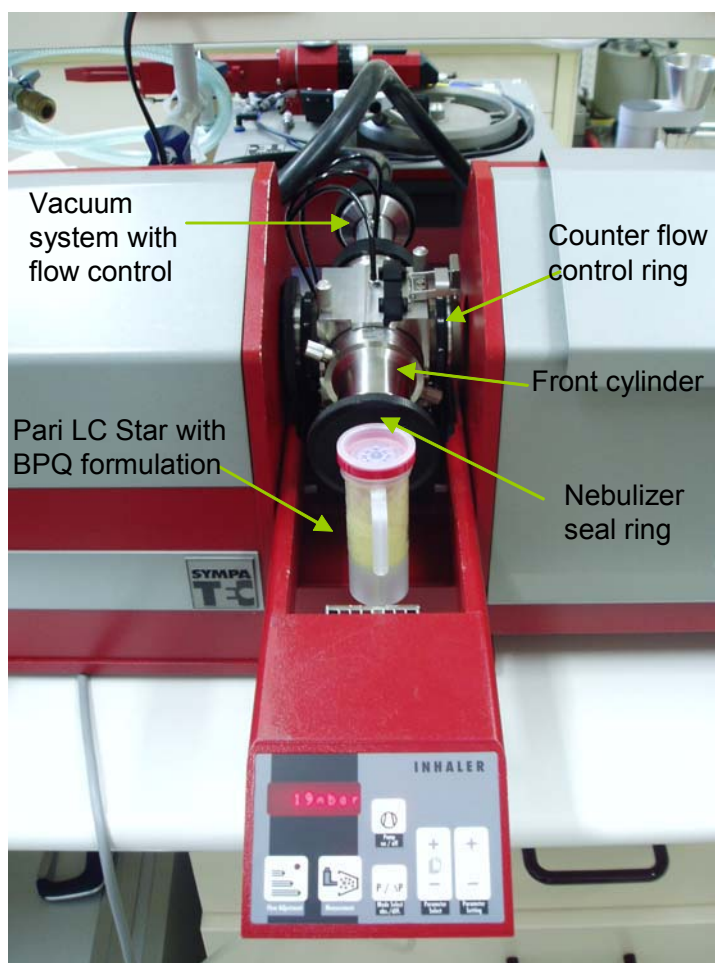


**Figure 3-15: Photograph of the laser diffraction apparatus Sympatec Helos BF/Magic<sup>®</sup>, with a modular inhaler adapter (INHALER<sup>®</sup>2000).**

### **3.2.3.3 Investigation of drug nanocrystals aggregation**

For achieving a controlled delivery to the lungs it is a pre-requisite that no uncontrollable crystal aggregation occurs. Ideally crystal aggregation should be absent. Therefore to judge the performance of a nebuliser, apart from analysis of the droplet sizes it is also essential to analyse the crystal size in the droplets after nebulization. To do this, the aerosol stream was directed towards the wall of a beaker and the condensed aerosol droplets collected. The suspension was then analysed by LD and PCS. The measurement of the drug nanocrystal aggregation performed during the first set of experiments is described in section 3.2.3.2, involving the sampling of the nanosuspension from the nebulizer reservoir at the beginning of the nebulization process, in the middle and at the end (0, 2.5 and 5 min) in order to compare these data with that obtained from the nanocrystals measured from the aerosol droplets collected. During the second set of experiments described in section

3.2.3.2, the aggregation potentially occurring was only investigated at the end of the nebulization process and compared to the initial size distribution of the drug nanocrystals.

#### **3.2.3.4 Drug output from jet nebulizers**

In the particular case of the nebulization of nanosuspensions, it is relevant to control the quantity of drug leaving the nebulizer. With suspensions, the laser diffraction device may describe a seemingly excellent particle size distribution without detecting that only a few of the particles measured, usually the larger ones, contain drug (O' Callaghan and Barry 1997). Although this situation has a very low probability when working with nanosuspensions, the influence of the drug formulation on the nebulizer drug output is of great interest, as the efficiency of the nebulization process is directly affected by the properties of the formulation such as viscosity and surface tension. In order to investigate this, 5 mL of nanosuspension were aerosolized until sputtering (time at which the nebulization flow is not continuous anymore) using a Pari LC Star nebulizer attached to a Pari-boy compressor. The time required was measured for each formulation and the drug residue in the nebuliser reservoir was recovered and quantified using a UV spectrophotometer  $\lambda=282$  nm (Apparatus Unicam UV 500 Thermo Spectronic). For the quantification of BPQ, as usual, the best-fit calibration line was determined each time by sum-squared linear regression analysis of the calibration data using five different concentration levels. The coefficient of correlation calculated for the method was  $r^2 = 0.9999$  within the calibration range (10-70  $\mu\text{g/mL}$ ). The drug was dissolved in using a mixture of ethanol-dimethylformamide 99:1 v/v. These studies were conducted in the *Department of Pharmaceutical Technology and Biopharmacy, University of Groningen Institute for Drug Exploration (GUIDE)*.

### **3.2.4 Methodology employed during the *in vivo* tests for the inhalation of buparvaquone nanosuspensions by *Pneumocystis pneumonia* infected mice**

The *in vivo* studies in order to test the inhalation of BPQ in infected mice were conducted at the *Cellular Immunology Unit P22 of the Robert Koch Institute* in Berlin (RKI). Tests and use of the animals were according the German law on animal protection and approved by the National Office for Safety at Work, Health Protection and Technical Safety (LaGetSi) in Berlin.

The limitations of this model for developing drug formulations ultimately for use in human pulmonary infections have been considered in this work. Unlike humans, rodents are compulsory nose breathers. Particles inhaled through the nose are less likely to reach the alveolar region than those inhaled through the mouth (oral inhalation in patients) due to the natural filter function of the nose (Raabe, Al-Bayati et al. 1988). Using intratracheal intubation to bypass the nose and thus enhance the number of particles reaching the lung, would have required anesthesia which, among other deficits, would have caused a reduction in the respiratory parameters (tidal volume and breathing frequency), as described by others (Rudolph, Ortiz et al. 2005). In this work, a whole body inhalation exposure chamber, especially designed for the production of aerosol droplets that pass the upper airways, was characterized and considered appropriate. A whole body chamber Glas-Col® Model A4224 (Glas-Col LLC, IN, USA) allows the mice to breathe freely, without the inevitable stress conditions encountered in a nose-only inhalation chamber (see chamber in Figure 3-12 page 64).

#### **3.2.4.1 Laboratory animals**

Previous groups have described the successful use of immunodeficient mice to test anti-*Pneumocystis* drugs (Walzer, Runck et al. 1997). The election of T- and B-cell-deficient mice as an experimental model to test the proposed BPQ formulation *in vivo*, as these mice are highly susceptible for spontaneous or induced infection with *P. murina*, typically developing high levels of pneumocystosis (Sidman and Roths 1994; Walzer, Runck et al. 1997).

Male immunocompetent C57BL/6 wild type (WT) mice (aged 6-8 weeks, weighing 22 ± 3 g) were used for determining the necessary drug aerosol exposure time (dose) in

the inhalation chamber. These animals were kept under conventional conditions (food and water available ad libidum) at the experimental animal facilities of the RKI. Female immunodeficient C57BL/6 *rag1*<sup>-/-</sup> (RAG) mice (aged 6-8 weeks, weighing 22 ± 2.5 g) lacking the recombination-activating gene-1, were used for infection with *P. murina*, establishing the PcP model, and for drug testing in randomly selected groups. These animals were housed in an individually ventilated cage system (EHRET BIO.A.S., Emmendingen, Germany), provided with sterile bedding, food and water (both given ad libidum), and handled under a class-II laminar air flow safety cabinet. Both mouse strains were bred and supplied by the animal breeding facility (ZVZ) of the Federal Institute for Risk Assessment (BfR), Berlin, Germany.

#### **3.2.4.2 Development of *Pneumocystis pneumonia* infection**

In this work, it was decided the use of mice which have become infected with *Pneumocystis* through natural environmental exposure, rather than by intratracheal or intranasal inoculation, because this mode of transmission is the natural mode of acquisition in humans and is almost certainly by the airborne route (Hughes 1982).

Four RAG mice (group A) received 3-7 × 10<sup>5</sup> partially purified *P. murina* microorganisms in 15 µl PBS by intranasal instillation. Five weeks later, a sentinel mouse was sacrificed to assess the progress of infection by excising the lung and doing optical and microscopical evaluation. Impression smears were prepared on glass slides, stained with DQ or BB, and analyzed under a conventional, respectively UV-fluorescence microscope. The presence of large aggregates (clusters) of trophozoites and cysts was taken as a sign of active infection. The remaining infected animals were used for passing the infection to 12 additional RAG mice (group B) by co-housing. Another three weeks later, this infection was also controlled by sacrificing a sentinel mouse from group B. Individual animals of group B now already showed first signs of pneumocystosis such as more rapid and labored breathing, rough fur, and a slight loss of weight. Finally, the remaining animals of group B were distributed among another 41 RAG mice (group C), further spreading the infection. Another three weeks later, a sentinel of this third group already had *Pneumocystis* trophozoites and cysts in the lung, confirming an ongoing PcP. Apart from the symptoms described above, some mice kept their eyes partially closed and their backs hunched. Together, these signs indicated the stage of moderate infection that had been aimed for to initiate the therapy.

### 3.2.4.3 Calculation of the dose inhaled and definition of inhalation exposure times

In order to have an approximation of the dose contained in the aerosol available for inhalation, the following calculations were done:

The concentration of BPQ available in the chamber after a given nebulization time was determined in the absence of animals by means of an ACI device. The general system settings were identical to those used later with animals. With a defined nebulization time, sampling time, and air volume, it was calculated that 0.3 mg of drug were present per liter of air per minute. Assuming that the volume of air inhaled by a mouse per minute is 0.070 liter (RMV, see below), it would inhale in 30 minutes a volume of 2.1 liters. Considering that only 67% of the BPQ particles are in the respirable aerosol fraction (< 3.3  $\mu\text{m}$ ), each mouse could inhale about 0.4 mg, corresponding to an aerosol dose of about 21 mg/kg body weight (assuming an average 20 g per mouse).

These approximations were used to calculate the “potential dose” inhaled by the animals during varying exposure times according the formula (Fukaya, Iimura et al. 2003):

$$\text{Dose (mg/kg)} = [\text{Concentration in the chamber (mg/l)} \times \text{RMV (l/min)} \times \text{D (min)} \times \text{F}] / \text{W (kg)}$$

where:

D = Duration of exposure to the compound

F = Proportion of inhalable particles (e.g. particles <3.3  $\mu\text{m}$ )

W = Body weight of the animals (~0.020 kg)

RMV = Rate of minute volume

The RMV value of 0.070 l/min was calculated according to information reported in the literature, which is based on plethysmographic measurements (Flandre and Desmecht; Flandre, Leroy et al. 2003). The reported mean tidal volume of 8 weeks old C57BL/6 male mice is 0.225 ml, and their mean respiratory frequency corresponds to 308.6 breaths/min.

In order to get a better understanding of the behavior and distribution of a certain inhaled dose of BPQ, a WT mouse was exposed to buparvaquone nanosuspension (BPQ-NS) aerosol for either 0.5, 1.5, 2.5, or 3.5 hours (this experiment was repeated

once). The animals were sacrificed approximately 45 minutes after the respective aerosol treatment and bled immediately. Organs were collected for determining the distribution of BPQ and for histological evaluation of the lung. Lung impression smears and lung cryo-sections were prepared from each animal and stained either with Diff-Quik® (DQ), bisbenzimidazole (BB), or hematoxylin and eosin (H&E) as described below.

#### **3.2.4.4 Test procedure for the drugs administration**

Forty *P. murina*-infected animals (group C, see above) were randomly divided into treatment and control groups of about 8 mice each. In the former, animals received treatment for 3 weeks on 5 days a week (Wednesdays and Sundays rest). Group 1 received no treatment and group 2 the aerosolized placebo. Group 3 received 20 mg BPQ-NS per kg mouse per os (gavage). Group 4 was exposed to aerosolized BPQ-NS for 30 minutes per day. Group 5 received 20 mg/kg ATQ formulated as a suspension per os (gavage). The mice were visited daily, weighed individually, and their food and water intake, general appearance, and activity monitored. All animals were sacrificed at the end of three weeks of therapy in order to determine the infection burden in the lungs.

#### **3.2.4.5 Histological and staining methods for microscopy**

Samples of lung tissue from all animals were fixed in 4% neutral-buffered *p*-formaldehyde (PFA) and embedded in paraffin blocks. Five micrometer sections were cut using a revolving microtome (RM2135, Leica, Bensheim, Germany) which were then deparaffinized and stained for microscopical analysis. Additionally, lung impression smears were prepared. For that, the left and right lungs of each mouse were split longitudinally and the fresh cuts gently pressed on glass slides. The preparations were air-dried and stained. Lung impression smears were stained either with Diff-Quik® (DQ) (Baxter, Unterschleissheim, Germany) or BisBenzimidazole H 33258 (BB) (Riedel-de Haën, Seelze, Germany) as previously described (Laube and Kiderlen 1998) for a quantitative microscopical assessment of the parasite burden. For investigating pathological changes in the lung tissue, paraffin sections were stained with DQ, BB, or with hematoxylin and eosin (H&E) (Accustain®, Sigma Aldrich, München, Germany) following standard procedure. Microscopical analysis of BB-stained preparations, was performed with a Zeiss Axioskop 2 equipped with fluorescence optics, a 365/12-nm excitation filter, and a 395-nm barrier filter (filter set

01; Zeiss), and using ×20, ×40, or ×100 oil immersion objectives. Photographs were obtained using an AxioCam digital camera and the AxioVision V 2.05 software (Carl Zeiss MicroImaging GmbH, Göttingen, Germany). The same microscope, only with conventional brightfield settings, was used for looking at the DQ- and H&E-stained preparations.

#### **3.2.4.6 Technique for estimating *Pneumocystis* burden in the lung**

Histologic and quantitative techniques of evaluation of therapy for experimental PcP were previously described in a rat model of pneumocystosis (Kim, Foy et al. 1987; Smulian, Linke et al. 1994). Longitudinal sections of the right and left lung were cut, placed in cold HBSS (Hank's balanced salt solution), frozen, and kept at -80 °C for two days. Then, the tissue was defrosted and homogenized by pressing it through a 70 µm nylon mesh cell strainer (BD Falcon™ BD Biosciences Europe, Erembodegem, Belgium) using the pistil of a 5 ml disposable syringe. The homogenate was centrifuged (228 x g, 7 min, 4°C), the supernatant transferred to a fresh tube, and washed two times with HBSS by centrifugation (2000 × g, 12 min, at 4°C). The pellet was then resuspended in 500 µl HBSS and 10 µl aliquots of this suspension or of serial dilutions thereof were dropped onto a glass slide which was stained with DQ or BB as described above. Diluting the homogenates allowed the *P. murina* trophozoite clusters to disaggregate somewhat, thus facilitating counting. For assessing the pathogens load, all microorganisms were counted microscopically in an oil immersion field (OIF) using a ×100 oil immersion objective were counted and multiple OIF were analyzed along the drop diameter. The total pathogens burden in each homogenate was calculated according to the formula:

$$\#Nuclei/ 500\mu l \text{ homogenate} = \#Nuclei \text{ per OIF} \times (\#OIF \text{ per drop diameter})^2 \times \text{dilution factor} \times 50$$

#### **3.2.4.7 HPLC method to quantify buparvaquone in mice plasma**

Mice were put to sleep by a brief inhalation of isofluran® (Baxter Deutschland GmbH, Erlangen, Germany), and then terminally bled by retroorbital puncture. Plasma samples were obtained by centrifugation. 100 µl aliquots of plasma were mixed with 25 µl of methanol-dimethylformamide (99:1) containing 100 µg/ml of parvaquone (2-cyclohexyl-3-hydroxy-1,4-naphthoquinone) (Cross Vetpharm Group Ltd, Dublin, Ireland) as internal standard. Parvaquone was chosen for its structural similarity

with BPQ. Samples were precipitated with 200  $\mu$ l acetonitrile-1.0% aqueous acetic acid (85:15 v/v), then centrifuged at 14,000 x g for 10 min. The supernatants were filtered using syringe disc filters fitted with a 0.20  $\mu$ m PTFE (polytetrafluoroethylene) membrane. 20  $\mu$ l of the filtrates were injected onto the chromatographic system (column and equipment as described in section 3.2.2.10). The detector wavelength was set at 280 nm. The calculation was based on the buparvaquone/parvaquone peak area ratio. Calibration samples were prepared by spiking negative murine plasma samples in the range from 0.5 to 50  $\mu$ g/ml. Blank plasma was used as a zero calibrator. The best-fit calibration line was determined each time by sum-squared linear regression analysis of the calibration data. The coefficient of correlation calculated for the method between the amount of drug spiked to the samples and the quantity recovered was  $r^2 = 0.9998$  within the calibration range. The limit of detection was determined as 0.5  $\mu$ g/ml. The drug recovery from spiked samples was 102.63%  $\pm$  12.63 (area ratio). The inter-assay precision expressed as coefficient of variation, ranged from 9.8% to 1.9% depending on the drug concentration.

#### **3.2.4.8 HPLC method to quantify buparvaquone in mice organs**

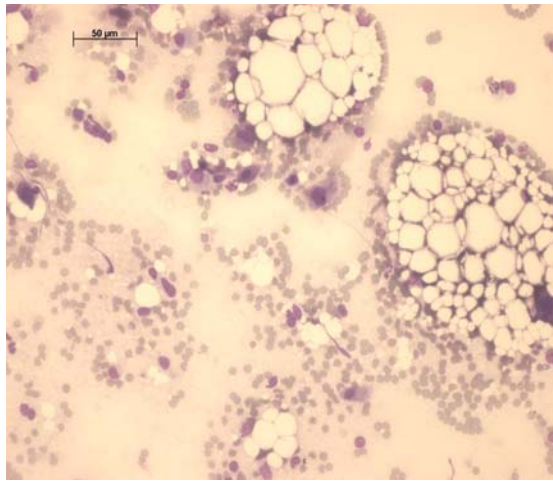
Selected organs were weighed and 50  $\mu$ l of an extraction solution consisting of hexane-isoamylalcohol 98:2 (v/v) (Hannan, Ridout et al. 1996; Hughes, Sillos et al. 1998) was added per mg tissue. Tissues were homogenized using an Ultra-Turrax (IKA T25 Janke-Kunkel, Staufen, Germany), at 22,000 rpm for 5-10 minutes, depending on the nature of the tissue, and then further dispersed on an automatic shaker (KL-2, Johanna Otto GmbH, Hechingen, Germany) for 20 min. The organic phase was separated from the debris by centrifugation (228 x g, 10 min, 4°C), and evaporated to dryness using a vacuum centrifuge (Bachofer Laboratoriumsgeräte, Reutlingen, Germany). The residues were mixed with 50  $\mu$ l of an internal standard solution (100  $\mu$ g parvaquone/ml) and 400  $\mu$ l mobile phase as described above with plasma. Samples were sonicated for 60 seconds, filtered through syringe disc filters fitted with a 0.20  $\mu$ m PTFE membrane, and 20  $\mu$ l of the filtrate were injected into the HPLC-system. Samples were analyzed at 280 nm calculating the drug concentration as a height ratio related to the internal standard peak. The drug recovery from spiked negative lung tissue ranged from 75 to 97% for 0.5 to 10  $\mu$ g/g.

### 3.2.4.9 Evaluation of drug activity

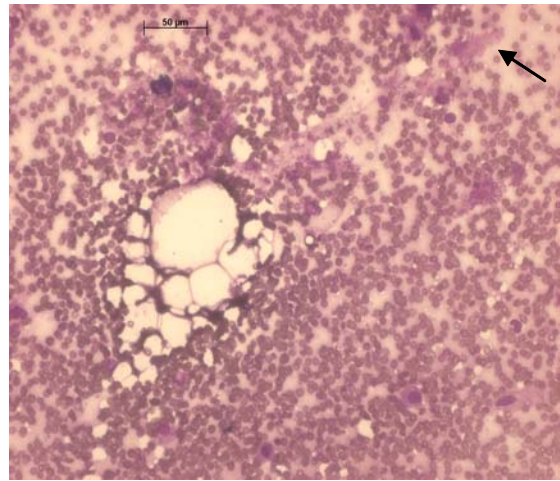
Anti-*P. murina* activity was primarily based on a reduction in the severity and extent of pneumocystosis in the lungs. Treatment efficacy was determined by comparing the *P. murina* burden in the treated groups with those in the controls in the same experiment. Pathogen counts were log transformed and compared by analysis of variance (one-way ANOVA) with Turkey's Post-Hoc test; statistical calculations were done either using the program SPSS v. 11.5 for windows or a worksheet prepared with Microsoft® Excel 2002. Significance was accepted when the P value was  $\leq 0.05$ . Efficacy of the treatment was also established by comparing infection rates as determined in BB-stained lung impression smears. The rates of infection were established based on the pathogens counted in 20 OIF (magnification 1000 $\times$ ), as follows: 0 = No parasites, 1 = 1-20, 2 = 21-30, 3 = 31-50, 4 = 50-90, and 5 = more than 90 pathogens.

In an additional approach, lung impression smears were stained with DQ. The abundance of clusters and microorganism aggregates as well as debris visualized by DQ, made it difficult to apply the same criteria as with BB. Therefore, the infection in individual samples was now estimated by visual comparison with five reference micro-photographs arbitrarily assigned to five different rates of infection (0 to 4). The Figure 3-16 shows representative photographs from each one of the infection rates defined. The photos were taken as representatives of the spectrum of infections previously observed with a  $\times 20$  objective.

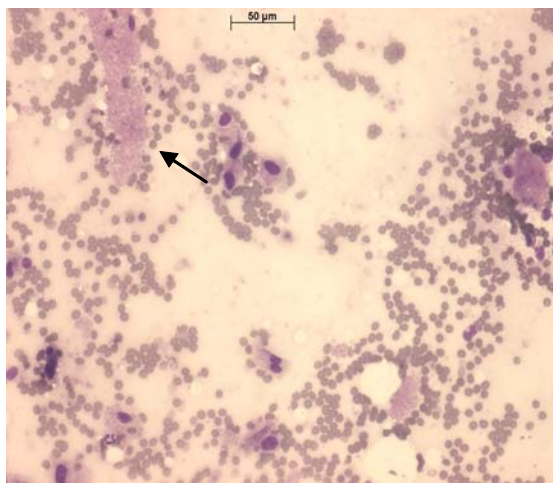
In either case, the data from lung impression smears were compared using the Kruskal-Wallis analysis of variance by ranks including a Dunn's post-Hoc test. Significant values were defined as P value  $\leq 0.05$ .



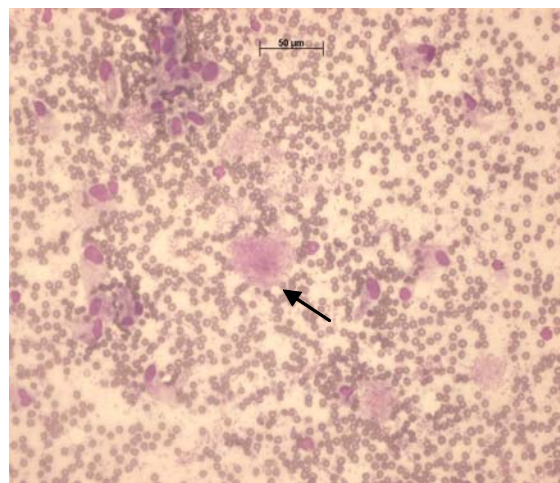
Infection rate = 0



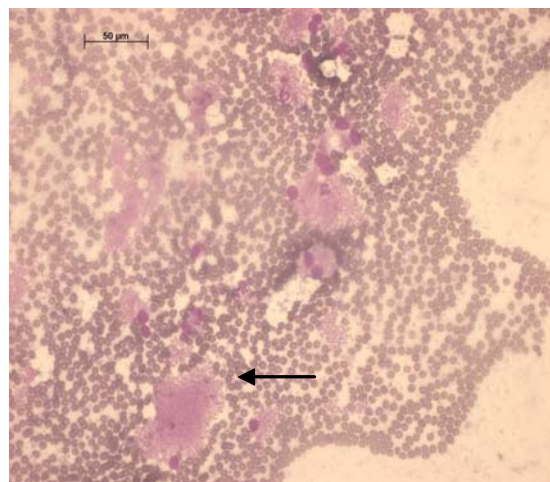
Infection rate = 1



Infection rate = 2



Infection rate = 3



Infection rate = 4

**Figure 3-16** Representative photos of the different infection rates (1 to 4) defined for the evaluation of the lung smears prepared from the 5 groups of treated animals. Arrows point *P. murina* trophozoites clusters. Diff-Quik<sup>®</sup> stain, 200× magnification.

### 3.2.5 Preparation of buparvaquone solid dispersions

One of the strategies to accelerate dissolution is the application of solid dispersions which consist of a rapidly dissolving hydrophilic matrix in which the lipophilic drug is distributed monomolecularly or in small particles. The conversion of the BPQ crystals into easily soluble powders with well defined shape and size should also allow the manufacture of a variety of dosage forms with good patient acceptance such as dry powders for inhalation (e.g. DPI's).

A solid dispersion is a type of formulation where the drug is dispersed in a solid carrier matrix. Depending on the method of manufacture of the solid dispersions and on the drug-carrier molecular interactions, an improvement in the dissolution rate is expected. The main well known reasons for achieving this effect are the formation of eutectic mixtures, where the drug is often present in a microcrystalline state, or due to a complete molecular dispersion of the amorphous drug in the carrier (formation of solid solutions). Other reasons involve for example a wettability effect of certain hydrophilic carriers, due to a close interaction with the surface of the lipophilic drug molecules as well as the ability of specific carriers to decrease the drug crystallinity (drug rearrangement in an amorphous state)(Hancock and Zografi 1997; Serajuddin 1999; Broman, Khoo et al. 2001).

Two different carriers were selected for this work: the hydrophilic synthetic polymer polyvinyl pyrrolidone (PVP), a GRAS additive with a broad range of applications related to its non-toxic nature and also to its solubility in both, water and organic solvents. The structure of PVP allows its interaction with hydrophobic as well as hydrophilic groups. The second carrier was inulin, a natural oligosaccharide extracted from plants. Inulin was chosen due to its non-toxicity and good physical stability (Hinrichs, Prinsen et al. 2001; van Drooge, Hinrichs et al. 2004). In addition, previous studies revealed that tablets prepared from inulin based solid dispersions showed excellent dissolution behavior (van Drooge, Hinrichs et al. 2004).

Solid dispersions described here were prepared basically by two different methods: The first method involved the dissolution of the drug in terbutyl alcohol (TBA) and mixing of this solution with a carrier solution (using water or TBA as a solvent) (van Drooge, Hinrichs et al. 2004). The mixing step was followed by a spray-freeze drying process in order to yield solid dispersion powders. The second method was the preparation of solid dispersions containing the drug in a nanocrystalline state. The base of this second method was the use of BPQ preformulated as nanocrystals

(Müller, Becker et al. 1999; Müller, Jacobs et al. 2001). The nanosuspension was mixed with a carrier aqueous solution and this mixture was subsequently either spray-freeze dried (SFD) or spray dried (SD). In either method, once the solid dispersion is exposed to aqueous media and the carrier dissolved, the drug was thought to be released as very fine colloidal particles, gaining surface area and increasing dissolution rate. The purpose of this work is to describe the physical characterization of the BPQ powders prepared, which lead to a better understanding of the molecular state and drug-carrier interactions and their relationship with the dissolution behaviour observed for the BPQ solid formulations. Solid dispersions described here were prepared at the *Department of Pharmaceutical Technology and Biopharmacy, University of Groningen Institute for Drug Exploration (GUIDE)*.

### **3.2.5.1 Spray drying process (SD)**

A Büchi 190 Mini Spray Dryer (Büchi, Flawil, Switzerland) equipped with a 0.5 mm two fluid nozzle was used. The peristaltic pump was set at number 2, the aspirator was set to number 10 (-30 mbar). The atomizing airflow was set at 800 L<sub>n</sub>/h and the heating was set to number 10. This combination of parameters yielded an inlet temperature of 150 ± 2 °C and an outlet temperature of 100 ± 2 °C. Samples were placed after collection in a vacuum desiccator over silica gel at room temperature at least one day before characterization.

### **3.2.5.2 Spray-freeze drying process (SFD)**

The mixture of drug/carrier to be processed was sprayed by means of a 0.5 mm two fluid nozzle (Büchi, Flawil, Switzerland) into liquid nitrogen. The liquid feed rate used during the spraying process was 10.5 mL/min and the atomizing air flow was 500 L<sub>n</sub>/h. In order to avoid freezing of the solution inside of the nozzle, hot water (about 90 °C) was pumped through the jacket of the nozzle. After evaporation of the liquid nitrogen the frozen droplets was freeze-dried using a Christ lyophilizer model Alpha 2-4 (Martin Christ Freeze Dryers GmbH, Osterode am Harz, Germany) with a condenser temperature of -53°C. The lyophilization procedure involved mainly two steps. First, the pressure was set at 0.220 mbar and the shelf temperature at -35 °C for the first 24 hours. During the second 24 hours, the shelf temperature was gradually raised to 20 °C while the pressure was decreased to 0.05 mbar. After removing the samples from the freeze drier, they were placed in a vacuum desiccator over silica gel at room temperature for at least another 24 hours. This procedure was

previously described for the preparation of fully amorphous sugar glass based solid dispersions (van Drooge, Hinrichs et al. 2004).

### **3.2.6 Characterization of buparvaquone solid dispersions**

#### **3.2.6.1 Scanning Electron Microscopy (SEM)**

Scanning electronic microscopy (SEM) pictures were taken with a JEOL JSM-6301F microscope (JEOL, Tokyo, Japan), using an acceleration voltage of 1.5 kV. Particles were scattered on double-sided adhesive tape on top of an aluminium specimen holder and subsequently coated with approximately 40-60 nm of gold/palladium, using a Balzers 120B sputter coater (Balzers AG, Liechtenstein). SEM pictures have been performed by Mr. Anko Eissens from the *Department of Pharmaceutical Technology and Biopharmacy, University of Groningen Institute for Drug Exploration (GUIDE)*.

#### **3.2.6.2 Temperature Modulated Differential Scanning Calorimetry (TMDSC)**

A differential scanning calorimeter DSC2920 (TA Instruments, Ghent, Belgium) was used to investigate the thermal behaviour of the solid dispersions. Indium was used for calibration of enthalpy ( $28.71 \text{ Jg}^{-1}$ ) and temperature ( $156.61^\circ\text{C}$ ). The samples, weighing 2-3 mg, were analysed in closed standard aluminium pans. The sample cell was continuously purged with nitrogen at a flow rate of 35 mL/min during the measurement. Residual moisture was removed from the samples by pre-heating them to a temperature of  $70^\circ\text{C}$  for 30 min before scanning was performed. The dried samples were scanned from 20 to  $250^\circ\text{C}$  at a rate of  $2^\circ\text{C}/\text{min}$ . Modulation conditions were set at amplitude of  $0.32^\circ\text{C}$  every 60 seconds period. The inflection point of the change in the reversing heat flow was taken as the glass transition temperature ( $T_g$ ). Measurements were performed at the *Department of Pharmaceutical Technology and Biopharmacy, University of Groningen Institute for Drug Exploration (GUIDE)*.

#### **3.2.6.3 X-Ray Powder Diffraction (XRPD)**

X-ray powder diffraction studies were conducted with an INEL CPS 120 diffractometer equipped with an  $120^\circ$  curved position sensitive detector and setup in Debye-Scherrer geometry. The detector allows simultaneous data collection in 4096 bins over a range of  $120^\circ$  in 2-theta. The x-ray source was a 1500W sealed tube with a Cu target used with a Ge (111) monochromator to give Cu K alpha 1 radiation

(Wavelength = 1.5406 Å). The sample holder was rotated about the axis defined by the planar surface of the sample to increase the number of crystallites in differing orientations contributing to the powder pattern, thus obtaining a better diffraction pattern. For the analysis of pure drug the powders have been mounted on a thin glass, being fastened to a brass pin without any previous sample treatment. Measurements were performed in collaboration with Mr. Klaus-J. Wenzel at the *Federal Institute for Materials Research and Testing (BAM)*.

#### **3.2.6.4 Dynamic Vapour Sorption (DVS)**

To investigate the water sorption properties of the solid dispersions, the water uptake was measured using a gravimetric sorption analyser DVS-1000 Water Sorption Instrument (Surface Measurement Systems Limited, London UK). Nitrogen was used as dried carrier gas, while water was selected as the source of vapour. Samples weighing 5-8 mg, were first dried by exposing them to 25°C and 0% relative humidity (RH). The study was performed in from 0 to 90% RH with steps of 10% RH. When the change of sample mass was less than 0.00050 wt. % per minute during a 10-min period, equilibrium was assumed and the humidity was changed to the next %RH stage until again equilibrium was reached. The amount of water absorbed was expressed as the mass percentage of water relative to the dry sample mass. Measurements were performed in collaboration with Mr. Anko Eissens from the *Department of Pharmaceutical Technology and Biopharmacy, University of Groningen Institute for Drug Exploration (GUIDE)*.

#### **3.2.6.6 In vitro dissolution behaviour**

In order to meet sink conditions, the dissolution medium consisted of a 2% polyoxyethylenesorbitan monolaurate (Tween 80) solution prepared with demineralised water. The pH of the dissolution medium was approximately neutral. 50 mg of the solid dispersion (containing 10 mg of drug) were tested in a vessel containing 500 mL of dissolution medium. All dissolution tests were performed using the rotating basket method, on a USP dissolution apparatus II (Rowa Techniek B.V., Leiderdorp, The Netherlands) at 50 rpm. Measurements were done in triplicate. BPQ concentration per vessel was measured every 2 min spectrophotometrically at 288 nm (Pharmacia LKB-Ultrospec III, Uppsala, Sweden). See calibration in section 3.2.2.9. Measurements were performed at the Department of Pharmaceutical

Technology and Biopharmacy, University of Groningen Institute for Drug Exploration (GUIDE).

### **3.2.6.7 Quantification of PVP during dissolution tests**

In order to quantify PVP, the specific samples were selected to test their dissolution behaviour using pure water instead of 2 % Tween 80 solution as dissolution medium to avoid the reaction interferences observed (data not shown). Samples were taken from the dissolution apparatus each 2 minutes for the first 10 minutes dissolution and subsequently each 30 min until 7 hours dissolution were monitored. For the quantification reaction, 1 mL dissolution medium were mixed with 2.6 mL of demineralised water and 0.72 mL of reagent. Samples were vortex shaken and measured in UV spectrophotometer Unicam UV 500 (Thermo Spectronic, Waltham, MA) at a wavelength of 432 nm. The reagent was composed of a mixture of 0.3184 g iodine, 22.29 g zinc sulphate (Sigma-Aldrich Chemie GmbH, Steinheim, Germany) and 1.802 g potassium iodide (Genfarma BV, Maarssen, The Netherlands) in 500 mL of demineralised water. Calibration curve in the range from 0.5 to 50 mg/500 mL The curve was done with seven concentration levels. The coefficient of correlation calculated for the method was  $r^2 = 0.9956$  within the calibration range.

(INTENTIONALLY BLANK)